IJC
International Journal of Cancer

Neddylation inhibition upregulates PD-L1 expression and enhances the efficacy of immune checkpoint blockade in glioblastoma

Shaolong Zhou[1]*, Xinyi Zhao[2]*, Zhuo Yang[1], Ruyi Yang[1], Chao Chen[1], Kailiang Zhao[3], Weiwei Wang[4], Yihui Ma[4], Qiang Zhang[2] and Xinjun Wang[1]

[1]Department of Neurosurgery, The Fifth Affiliated Hospital of Zhengzhou University, Zhengzhou, Henan, China
[2]Department of Radiation Oncology, University of Michigan Medical School, Ann Arbor, MI
[3]Department of General Surgery, Renmin Hospital of Wuhan University, Wuhan, Hubei, China
[4]Department of Pathology, The First Affiliated Hospital of Zhengzhou University, Zhengzhou, Henan, China

Pevonedistat (MLN4924), a specific NEDD8-activating enzyme inhibitor, has been considered as a promising treatment for glioblastoma, which is currently in Phase I/II clinical trials. On the other hand, inhibition of neddylation pathway substantially upregulates the expression of T cell negative regulator programmed death-ligand 1 (PD-L1), which might account for the potential resistance *via* evasion of immune surveillance checkpoints. Whether administration of anti-PD-L1 enhances the efficacy of pevonedistat through a cytotoxic T cell-dependent mechanism in glioblastoma needs to be investigated. Here, we report that depletion of neddylation pathway key enzymes markedly elevates PD-L1 expression in glioblastoma cancer cells. Consistently, neddylation inhibitor pevonedistat significantly enhances PD-L1 expression in both glioblastoma cancer cell lines and animal models. Mechanistically, pevonedistat increases *PD-L1* mRNA levels mainly through inhibiting Cullin1-F-box and WD repeat domain-containing 7 E3 ligase activity and accumulating c-MYC proteins, a direct transcriptional activator of *PD-L1* gene expression. In addition, inhibition of Cullin3 activity by pevonedistat also blocks PD-L1 protein degradation. Importantly, pevonedistat attenuates T cell killing through PD-L1 induction, and blockade of PD-L1 restores the sensitivity of pevonedistat-treated glioblastoma cancer cells to T cell killing. The combination of pevonedistat and anti-PD-L1 therapy compared to each agent alone significantly increased the therapeutic efficacy *in vivo*. Our study demonstrates inhibition of neddylation pathway suppresses cancer-associated immunity and provides solid evidence to support the combination of pevonedistat and PD-L1/programmed cell death protein 1 immune checkpoint blockade as a potential therapeutic strategy to treat glioblastoma.

Introduction

Glioblastoma multiforme (GBM), arising from malignant glial cells (such as astrocytes and oligodendrocytes), is the most common and lethal form of brain tumor. In addition, GBM accounts for more than half of all primary brain tumors.[1] Despite survival benefits have been improved by current treatment, median survival remains just only more than 1 year (12~15 months) after standard surgery followed by fractionated radiotherapy and temozolomide.[2] Since GBM is frequently refractory to current chemotherapy/radiotherapy regimes, there is a dire need to improve treatment options for GBM.

Protein neddylation is a post-translational modification process by which the ubiquitin-like protein NEDD8 is conjugated to its target proteins.[3] This process is catalyzed by three enzymes in a

Key words: pevonedistat, neddylation, immunotherapy, PD-L1, glioblastoma

Abbreviations: ChIP: chromatin immunoprecipitation; FACS: fluorescence assisted cell sorting; FBXW7: F-box and WD repeat domain-containing 7; GBM: glioblastoma multiforme; IHC: immunohistochemistry; NED: NEDD8-activating enzyme; PBMC: peripheral blood mononuclear cell; PD-1: programmed cell death protein 1; PD-L1: programmed death-ligand 1; RFP: red fluorescent protein

Additional Supporting Information may be found in the online version of this article.

Conflict of interest: No potential conflicts are disclosed in this study.

Grant sponsor: Key Research Projects of Henan Higher Education Institutions, China; **Grant number:** 14A320078; **Grant sponsor:** National Natural Science Foundation of China; **Grant number:** 81874068

*S.Z. and X.Z. contributed equally to this work

DOI: 10.1002/ijc.32379

History: Received 2 Jan 2019; Accepted 18 Apr 2019; Online 1 May 2019.

Correspondence to: Xinjun Wang, Department of Neurosurgery, the Fifth Affiliated Hospital of Zhengzhou University, Kangfu-qian Street No. 3, Zhengzhou, Henan Province 450052, China, Tel.: 86-371-66916754, Fax: 86-371-66916754, E-mail: wangxj@zzu.edu.cn; or Qiang Zhang, Department of Radiation Oncology, University of Michigan, 4320 MS1, Ann Arbor, MI 48109, USA, Tel.: 734-764-3324, Fax: 734-763-1581, E-mail: qiangz@med.umich.edu

What's new?

Inhibitors of neddylation, a posttranslational modification that adds the ubiquitin-like NEDD8 protein to target proteins, are promising cancer therapeutics, but might enhance cancer-associated immunosuppression. Here the authors show that neddylation inhibitor pevonedistat upregulates programmed death ligand 1 (PD-L1) expression on glioblastoma cell lines through stabilization of the c-Myc transcription factor. Blockade of the PD-L1/PD-1 interaction potentiates the effect of pevonedistat on glioblastoma cell survival, providing proof-of-concept evidence for combining pevonedistat and PD-L1/PD-1-blocking antibodies in future clinical trials.

sequential action: the E1 NEDD8-activating enzyme (NAE), consisting of NAE1 (APP-BP1) and UBA3 (ubiquitin like modifier activating enzyme 3) heterodimer; the E2 NEDD8-conjugating enzymes (UBC12/UBE2M and UBE2F) and the E3 NEDD8 ligases.[4] The neddylation pathway has been identified to be overactivated in a majority of GBM tumor tissues compared to normal tissues.[5] Pevonedistat (MLN4924) is a first-in-class NAE inhibitor, which has been recently considered as an attractive anticancer agent and has shown a significant therapeutic effect in some Phase I clinical cancer trials.[6,7] Pevonedistat treatment largely blocks cullin neddylation and inhibits cullin-RING E3 ligase activity, and in turn leads to the accumulation of tumor suppressor substrates to induce cell-cycle arrest, senescence or apoptosis in GBM cells. Additionally, pevonedistat orthotopically suppressed tumor growth in a xenograft model of human GBM.[5] Several combinations of pevonedistat and anticancer agents have been proposed to enhance the cytotoxic effect of pevonedistat.[8–12] Thus, developing a rational combination therapy with pevonedistat may improve anticancer strategy.

In the past decade, some major breakthroughs have been achieved in our understanding of cancer cell immunosuppression. Multiple inhibitory ligands expressed on the surface of tumor cells, notably programmed death-ligand 1 (PD-L1), are shown to be key molecules in cancer immune evasion. Interaction of PD-L1 with the programmed cell death protein 1 (PD-1) receptor on T cells leads to reduced T cell proliferation, cytolytic activity and cytokine release. Therefore, PD-1/PD-L1 antibodies block the co-inhibitory ligation and restore T cell function.[13,14] The checkpoint blockade immunotherapies (such as nivolumab and atezolizumab) have been approved by FDA for the treatment of multiple types of cancer.[15,16] In GBM, higher PD-L1 expression has been correlated with poorer patient prognoses,[17] suggesting that PD-L1 does suppress antitumor immunity in some patients. In addition, case reports have indicated that anti-PD-1 therapy is effective for some patients with GBM.[18] A few of ongoing clinical trials, including nivolumab monotherapy as well as combination with temozolomide or radiotherapy, are exploring the efficacy across different lines of treatment in GBM patients.

Accumulating evidence demonstrates that some conventional and targeted cancer therapies modulate antitumor immunity,[19,20] suggesting combination of cytotoxic anticancer agents with immune checkpoint blockade treatment might lead to promising combinatorial regimens. In the current study, we find genetic and pharmacologic inhibition of neddylation pathway significantly increases PD-L1 expression in GBM cancer cells. Protein neddylation inhibitor pevonedistat enhances PD-L1 transcription by inactivating SKP1-Cullin1-F-box and WD repeat domain-containing 7 (FBXW7) activity and blocking c-MYC protein degradation, which turns on *PD-L1* gene expression. In line with this observation, coadministration of pevonedistat and anti-PD-L1 antibody induces synergistic effect in suppression of GBM cancer cell growth in an animal model. Thus, our work presents a proof-of-concept study for the evaluation of PD-L1/PD-1 blockade with pevonedistat in GBM.

Methods

Cell lines, cultures and reagents

Human GBM cell lines U87, the stable red fluorescent protein (RFP) expressing U87 cells, T98G cells and mouse glioma GL261 cells were obtained from the American Type Culture Collection (ATCC, Manassas, VA, USA), and cultured in Dulbecco's Modified Eagle's Medium (Hyclone, Logan, UT, USA) containing 10% fetal bovine serum (Biochrom AG, Berlin, Germany) and 1% penicillin/streptomycin solution at 37°C with 5% CO_2. All cell lines were tested and free of mycoplasma contamination. MG132 were dissolved in dimethyl sulfoxide. For *in vitro* studies, pevonedistat was dissolved in dimethyl sulfoxide, while pevonedistat was freshly dissolved in 10% HPBCD (2-hydroxypropyl-β-cyclodextrin) and stored in dark for *in vivo* studies.

Antibodies and immunoblotting

For direct Western blotting analysis, cells were lysed in RIPA buffer with proteinase and phosphatase inhibitors. The antibodies used were as follows: human PD-L1 (Cell Signaling, Beverly, MA), mouse PD-L1 (R&D Systems, Minneapolis, MN, USA), NEDD8 (Cell Signal, Beverly, MA), NAE1 (Sigma, St. Louis, MO, USA), UBA3 (Epitomics, Inc., Burlingame, CA, USA), UBE12/UbE2M (Abcam, Cambridge, MA, USA), Cullin1 (Santa Cruz Biotechnology Inc., Santa Cruz, CA, USA), Cullin3 (Cell Signal, Beverly, MA), FBXW7 (Bethyl Laboratories, Montgomery, TX, USA), c-MYC (Cell Signaling, Beverly, MA), FLAG (Sigma, St. Louis, MO, USA) and β-actin (Santa Cruz Biotechnology Inc., Santa Cruz, CA, USA).

RNA isolation, first strand cDNA synthesis and RT-qPCR

Total RNA was isolated from cells using the RNeasy Mini Kit (Qiagen, Hilden, Germany). cDNA was obtained by reverse transcription using the Maxima First Strand cDNA Synthesis Kit for RT-qPCR (Thermo Fisher Scientific), according to the manufacturer's

instructions. Relative mRNA levels were normalized to GAPDH mRNA levels. Primer sets used were as follows: *CD274*-Forward: ATTTGGAGGATGTGCCAGAG; *CD274*-Reverse: CCAGCACA CTGAGAATCAACA; *GAPDH*-Forward: AAGGTGAAGGTCG GAGTCAA; *GAPDH*-Reverse: AATGAAGGGGTCATTGATGG.

Cell surface PD-L1 detection

Cells were trypsinized and resuspended in 100 μL of cell staining buffer (#420201, BioLegend, San Diego, CA, USA) and incubated with APC-conjugated anti-human PD-L1 antibody (#329708, BioLegend) for 1 hr at room temperature. Stained cells were washed in the staining buffer and analyzed by fluorescence assisted cell sorting (FACS) (BD Biosciences). The PD-L1 expression levels on the cell surface were analyzed in FlowJo 7.6.

ChIP assay

U87 cells were treated with or without pevonedistat for 48 hr and fixed by adding formaldehyde (Fisher) into the culture medium to a final concentration of 1%. Cross-linking was allowed to proceed for 15 min and stopped by addition of glycine (0.125 M). Fixed cells were washed with PBS and resuspended in IP Buffer (100 mM Tris at pH 8.6, 0.3% SDS, 1.7% Triton X-100 and 5 mM EDTA). Cells were sonicated with a 1/4-inch-diameter tapered probe for 30 sec in a Branson 250 sonicator to produce genomic DNA fragments (100~400 bp). Samples were immunoprecipitated overnight at 4°C with polyclonal antibody specific for c-MYC (2 μg N262, Santa Cruz) and protein A beads. Beads were washed/eluted and phenol/chloroform-extracted and ethanol-precipitated. DNA was resuspended in 100 μL of water and applied for qPCR analysis. *PD-L1* promoter DNA fragment enrichment was analyzed by qPCR. *PD-L1* promoter primers for qPCR-Forward: GCTTTAATCTTCGAAACTCTTCCC, Reverse: CCTAGGAAT AAAGCTGTGTATAGAAATG.

In vivo ubiquitination assay

The U87 cells were transfected with His-ubiquitin and FLAG-PD-L1 as well as scramble or Cullin3 siRNA. 48 hr post-transfection, cells were treated with 10 μM MG132 for 4 hr and lysed in buffer A (6 M guanidine-HCl, 0.1 M Na_2HPO_4/NaH_2PO_4 and 10 mM imidazole [pH 7.5]). After sonication, the lysates were incubated with Ni-NTA beads (QIAGEN) for 4 hr at room temperature. The His pull-down proteins were washed twice with buffer A and then twice with buffer A/B (1 volume buffer A and 3 volumes buffer B), and one time with buffer B (25 mM Tris–HCl and 20 mM imidazole [pH 6.8]). The pull-down samples were resolved by 2 × SDS-PAGE for immunoblotting.

PD-1 binding assay

The U87 and T98G cells were treated with or without pevonedistat for 48 hr, then cells were trypsinized and incubated with 2 μg/mL recombinant human PD-1 FC chimera protein (#1086-PD-050, R&D Systems, Minneapolis, MN, USA) at room temperature for 30 min. Cells were extensively washed in staining buffer and further incubated with anti-human Alexa Fluor 488 dye conjugated antibody (Thermo Fisher Scientific) at room temperature for 30 min. Cells were analyzed by FACS after wash in the staining buffer, and the FACS data were analyzed using FlowJo 7.6.

T cell killing assay

The U87-RFP human glioma cells were seeded in a 24-well plate with or without pevonedistat for 24 hr. Human peripheral blood mononuclear cells (PBMC; #70025, STEMCELL, Vancouver, WA, Canada) were activated with CD3 antibody (50 ng/mL), CD28 antibody (50 ng/mL), and IL2 (10 ng/mL) (#317303; #302913; #589102, BioLegend) and then co-cultured with U87-RFP cells at 10:1 ratio. After 24 hr, U87-RFP cells were sorted by FACS and subjected to clonogenic assay. After 10 days, the colonies were stained with 0.5% crystal violet and counted using a stereomicroscope.

Xenograft studies

All animal studies were approved by Zhengzhou University Animal Care and Use Committee and performed in accordance with guidelines. U87 or T98G (2×10^6) cells were injected into the bilateral dorsal flanks of female nude mice (6–8 weeks). When tumor volume reached approximately 60 mm^3, mice were administered pevonedistat i.p. at a dose of 30 mg/kg 5 days per week for 3 weeks (as shown in Fig. 2*a*). Tumors were collected after final treatment and applied for immunoblotting and immunohistochemistry (IHC) analysis.

IHC staining of tumor tissue samples

U87 and T98G xenografted tumors in nude mice were formalin-fixed, embedded in paraffin. Sections of 4-μm thick were cut and incubated with 3% H_2O_2 for 15 min at room temperature to block endogenous peroxidase activity. After incubating in normal goat serum for 1 hr to block nonspecific binding of IgG, sections were treated with primary antibody (PD-L1, clone E1L3N, Cell Signaling) at 4°C overnight. Sections were then incubated for 30 min with biotinylated goat-anti-mouse IgG secondary antibodies (Fuzhou Maixin Biotech, Fuzhou, Fujian, China), followed by incubation with streptavidin-conjugated HRP (Fuzhou Maixin Biotech) and were developed with 3,3′-diaminobenzidine (Fuzhou Maixin Biotech). Images were taken using an Olympus microscopic camera and matched software. To analyze and measure the IHC PD-L1 expression from U87 and T98G xenografts, the stained slides were digitally scanned using the Aperio ScanScope AT2 slide scanner (Leica Biosystems, Wetzlar, Germany) and were captured with a 20× objective. The images were visualized using ImageScope software (Leica Biosystems) and analyzed by two pathologists (W.W. and Y.M.) using Aperio Image Toolbox analysis software (Leica Biosystems). Cellular membranous PD-L1 IHC expression on U87 and T98G xenografted tumor cells was considered as positive PD-L1 expression. The intensity scored as 0 (no staining), 1+ (weak staining), 2+ (moderate staining), 3+ (strong staining) and extension (percentage) of

expression were determined in each image. PD-L1 H-score from each image was determined by multiplying the staining intensity and the percentage of positive cells (a range of 0–300).

IHC analysis for Ki-67 was performed on the formalin-fixed paraffin-embedded allograft samples with anti-Ki-67 rabbit monoclonal antibody (mAb) (30-9, Ventana, Tucson, AZ, USA). Five randomly selected, nonoverlapping images (20× objective) were acquired for each specimen (three independent animals per genotype). Ki-67-positive cells and total cells were manually counted for each image, and the staining was quantified by calculation the percentage of Ki-67 positive cells.

PD-L1 antibody and pevonedistat treated syngeneic tumor model

C57BL/6 mice (6–8-week-old female) were subcutaneously injected with 1×10^7 GL261 cells. Seven days after the injection of tumor cells, mice were randomly divided into four groups with comparable average tumor size: IgG control antibody treatment, pevonedistat treatment, αPD-L1 treatment and pevonedistat plus αPD-L1 treatment. Mice were injected intraperitoneally with 15 mg/kg pevonedistat or vehicle daily for a total of 15 injections. In addition, 75 μg anti-mouse PD-L1 antibody (10F.9G2, Bio X Cell, West Lebanon, NH, USA) or control rat IgG2b (LTF-2, Bio X Cell) were injected intraperitoneally every 4 days for a total of 5 injections (as shown in Fig. 5*a*). Tumor volumes were measured every 4 days and were calculated using the formula: length × width^2 × 0.5. Statistical analysis was conducted using the GraphPad Prism software.

Statistical analysis

All data are represented as the mean ± SD. The statistical significance of differences between groups was assessed using GraphPad Prism6 software with the Student *t*-test or one-way ANOVA. The unpaired two-tailed *t*-test was used for comparing parameters between groups. Three levels of significance ($^*P < 0.05$, $^{**}P < 0.01$ and $^{***}P < 0.001$) were used for all tests.

Results

Genetic or pharmacological inhibition of neddylation pathway enhances PD-L1 expression *in vitro*

To determine whether inhibition of neddylation pathway affects PD-L1 protein level in GBM cells, we treated U87 and T98G cells with siNAE1, siUBA3 or siUBC12, and determined PD-L1 protein expression by immunoblotting. Depletion of neddylation pathway enzymes NAE1, UBA3 or UBC12 markedly increased the total level of PD-L1 in both cell lines (Fig. 1*a* and Fig. S1*a*). Mature PD-L1 expressed at the surface of cancer cells exerts immunosuppressive effects by binding to PD-1 glycoprotein receptor on activated T cells.[21] To further determine whether the cell surface PD-L1 level is upregulated upon silencing of these neddylation pathway enzymes, cells transfected with non-targeting siRNA, siNAE1, siUBA3 or siUBC12 were subjected to flow cytometry using fluorescence-labeled PD-L1 antibody. Knocking down of any individual neddylation enzymes significantly elevated the cell surface PD-L1 levels in both human GBM cell lines (Fig. 1*b* and Fig. S1*b*). The key physiological substrates of neddylation are cullin family numbers, which regulate hundreds of protein stability, including PD-L1.[22] Interestingly, the mRNA of *PD-L1* was upregulated after cells were depleted of neddylation enzymes, indicating inhibition of neddylation pathway also transcriptionally increases PD-L1 levels (Fig. 1*c* and Fig. S1*c*). In addition, in the murine GBM cell line GL261, we also assessed PD-L1 protein level upon silencing of neddylation pathway enzymes. Neddylation enzyme-depleted GL261 cells exhibited higher PD-L1 expression compared to control cells (Fig. 1*d*).

Pevonedistat, the neddylation pharmacological inhibitor, forms a covalently bound adduct with NEDD8 while bound to NAE and inhibits protein neddylation.[6,23] In order to examine the effect of pevonedistat on PD-L1 protein levels, we treated U87 cells with either pevonedistat or proteasome inhibitor MG132. Both inhibitors markedly increased the overall protein level of PD-L1 (Fig. 1*e*). Consistent with the results, pevonedistat and MG132 are both able to elevate cell surface PD-L1 levels in U87 and T98G cells (Fig. 1*f* and Fig. S1*d*). Interestingly, in line with the neddylation enzyme depletion results, pevonedistat induced *PD-L1* mRNA levels in both the cell lines, while MG132 treatment did not show any significant changes in *PD-L1* transcripts (Fig. 1*g*). The similar effect of pevonedistat on murine GL261 cells was shown in Figure 1*h*. Together, these results indicated that genetic and pharmacologic inhibition of the neddylation pathway upregulates PD-L1 expression in GBM cells.

Pevonedistat enhances PD-L1 expression *in vivo*

We next sought to examine whether pevonedistat may affect PD-L1 expression in tumors. Mice bearing U87 and T98G cells were treated with pevonedistat 5 days a week for 3 weeks (Fig. 2*a*). Tumor tissues from xenografts were harvested and subjected to qPCR analysis for the expression of *PD-1* mRNA and immunoblotting with PD-L1 antibody. As shown in Figure 2*b* and Figure S2*a*, *PD-L1* mRNA levels were significantly elevated upon pevonedistat treatment in U87 and T98G xenografts as compared to control. Consistently, PD-L1 protein levels are much higher in the pevonedistat-treated tumors compared to control tumors (Fig. 2*c* and Fig. S2*b*). In line with the results, we also found increased PD-L1 protein staining in the tumors from mice administered with pevonedistat relative to untreated tumors (Figs. 2*d* and 2*e*; Figs. S2*c* and S2*d*). These *in vivo* results substantially support the conclusion that inhibition neddylation pathway by pevonedistat leads to PD-L1 upregulation in GBM tumors.

Cullin1-FBXW7/c-MYC axis mainly contributes to the PD-L1 induction in GBM cells

The cullin family members of cullin-RING Ligases are the major substrates for NEDD8 conjugation (neddylation).[24,25] Zhang and colleagues recently investigated the potential interaction between

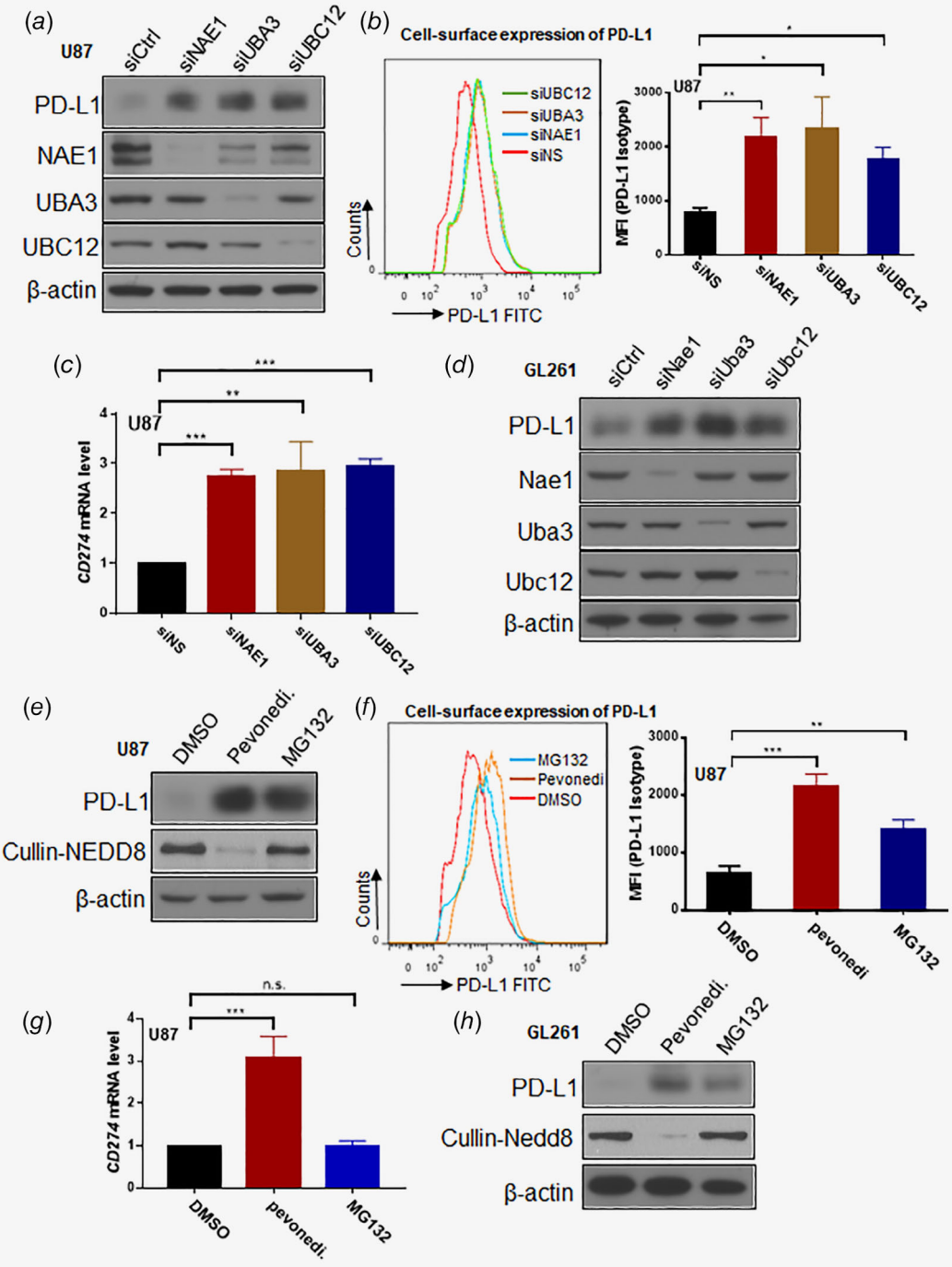

Figure 1. Inhibition of neddylation pathway increases PD-L1 expression in glioblastoma cells *in vitro*. (*a*) Depletion of neddylation pathway enzymes (NAE1, UBA3 or UBC12) markedly increased PD-L1 protein levels in U87 cells. (*b*) The U87 cells treated with NAE1, UBA3 or UBC12 siRNA were subjected to FACS analysis for cell surface PD-L1 expression. (*c*) Silencing of neddylation pathway enzymes upregulates *PD-L1* mRNA expression. (*d*) Mouse glioma GL261 cells were transfected with siRNA targeting Nae1, Uba3 or Ubc12 for 72 hr. Mouse PD-L1 protein levels were detected by Western blotting. (*e*) U87 cells were treated with pevonedistat (1 μM) or MG132 (1 μM) for 24 hr. PD-L1 protein was examined by Western blotting. (*f*) Cell-surface expression of PD-L1 was examined by using flow cytometry upon treatment with pevonedistat or MG132 (left), and the quantification of PD-L1 expression was shown (right). (*g*) *PD-L1* mRNA expression was analyzed by qPCR in U87 cells treated with pevonedistat or MG132 for 24 hr. (*h*) PD-L1 was upregulated in GL261 cells with either pevonedistat or MG132 treatment. [Color figure can be viewed at wileyonlinelibrary.com]

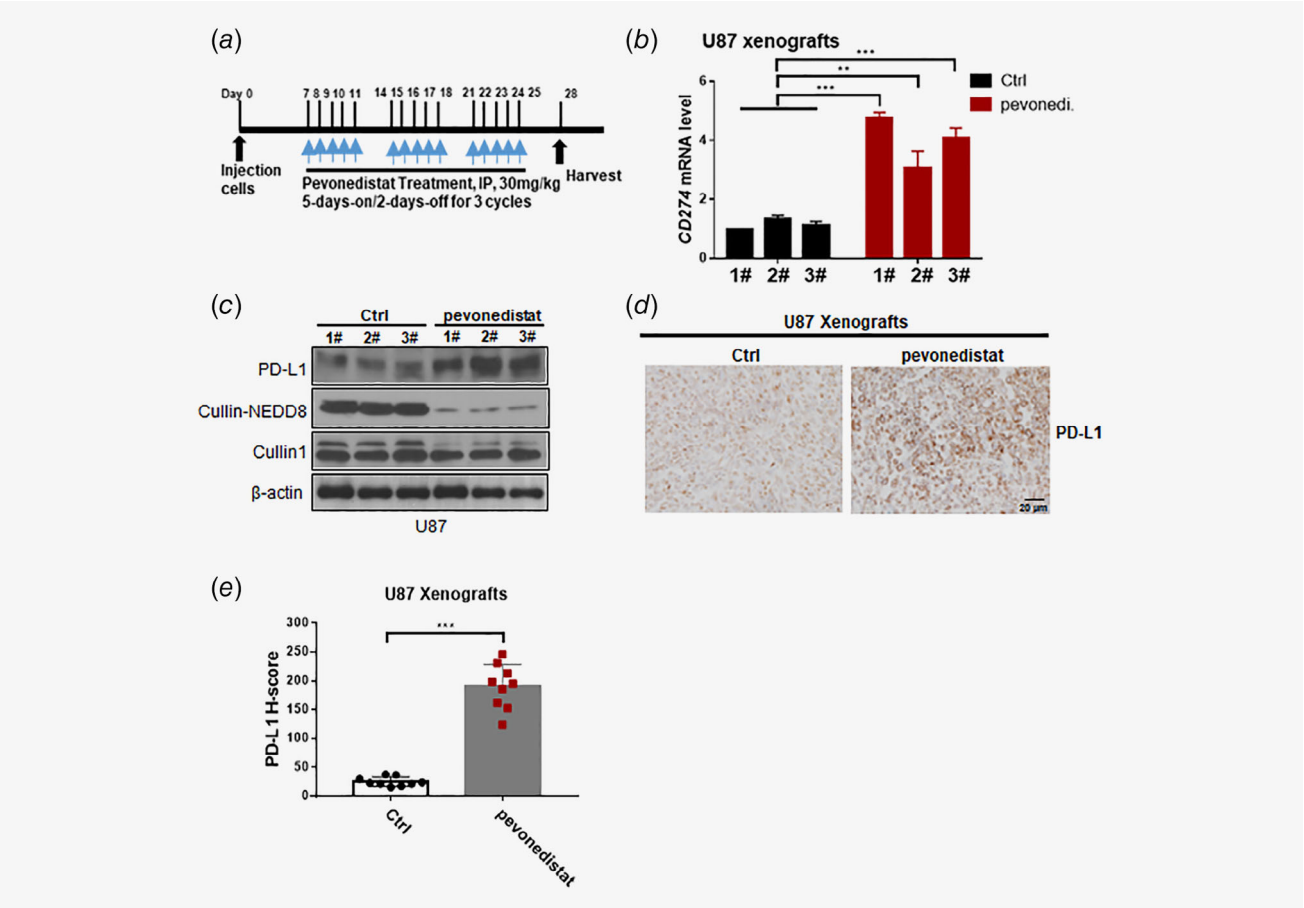

Figure 2. Neddylation inhibitor pevonedistat induces PD-L1 expression in vivo. (*a*) A schematic of the treatment plan for nude mice bearing subcutaneous U87 tumors. Female nude mice were implanted with 1×10^7 U87 cells subcutaneously and received neddylation inhibitor pevonedistat treatment. (*b*) Human *PD-L1* mRNA expression was analyzed by qPCR in U87 xenografts treated with pevonedistat or vehicle. (*c*) U87 tumors were isolated, and total proteins were prepared to evaluate PD-L1 expression by immunoblotting. (*d*, *e*) U87 tumors were also subjected to IHC for the detection of PD-L1 and quantification for PD-L1 staining. Scale bar, 20 μm. [Color figure can be viewed at wileyonlinelibrary.com]

cullin protein and PD-L1. They found that PD-L1 is able to bind to both Cullin1 and Cullin3, but the interaction is stronger with Cullin3.[22] Thus, we detected the PD-L1 protein levels upon silencing of Cullin1 or Cullin3. Consistently, we observed higher protein levels of PD-L1 in both Cullin1- and Cullin3-depleted U87 and T98G cells (Fig. 3*a* and Fig. S3*a*). Surprisingly, we found much higher upregulation of PD-L1 in the cells with silencing of Cullin1 relative to that in the cells with Cullin3 knockdown (Fig. 3*a* and Fig. S3*a*). Similar results were observed for the PD-L1 protein levels on the cell surface in both cell lines, which support the conclusion that PD-L1 expression is associated with Cullin1 protein levels in GBM cells (Fig. 3*b* and Fig. S3*b*). The half-life of oncoprotein c-MYC is mainly regulated by Cullin1-FBXW7 E3 ligase, and importantly c-MYC is recently identified as a key transcriptional activator of *PD-L1* gene by directly binding to *PD-L1* promoter region.[26] Therefore, we next examined the effect of FBXW7 depletion on PD-L1 mRNA and protein levels in two GBM cell lines. As expected, knockdown of FBXW7 led to the accumulation of c-MYC oncoprotein, as well as the elevation of PD-L1 mRNA and protein levels in both U87 and T98G cells (Figs. 3*c* and 3*f*). In line with these results, depletion of FBXW7 also elevated the protein abundance of cell surface PD-L1 (Figs. 3*g* and 3*h*). Moreover, we used chromatin immunoprecipitation (ChIP) to evaluate c-MYC-dependent *PD-L1* gene transcription upon FBXW7 silencing. As shown in Figure 3*i*, the binding of c-MYC to the *PD-L1* promoter region was significantly increased in siFBXW7-treated U87 cells relative to control cells.

To further explore whether the negative regulation of PD-L1 expression by FBXW7 is through c-MYC, we co-transfected the U87 cells with FBXW7 and c-MYC siRNAs and examined the total and cell surface PD-L1 protein levels by immunoblotting and flow cytometry. In support of our hypothesis, depletion of c-MYC markedly abrogated the upregulation of both PD-L1 mRNA and protein in FBXW7-knocked down cells (Figs. 3*j* and 3*l*). Consistent with the results in U87 cells, similar effect

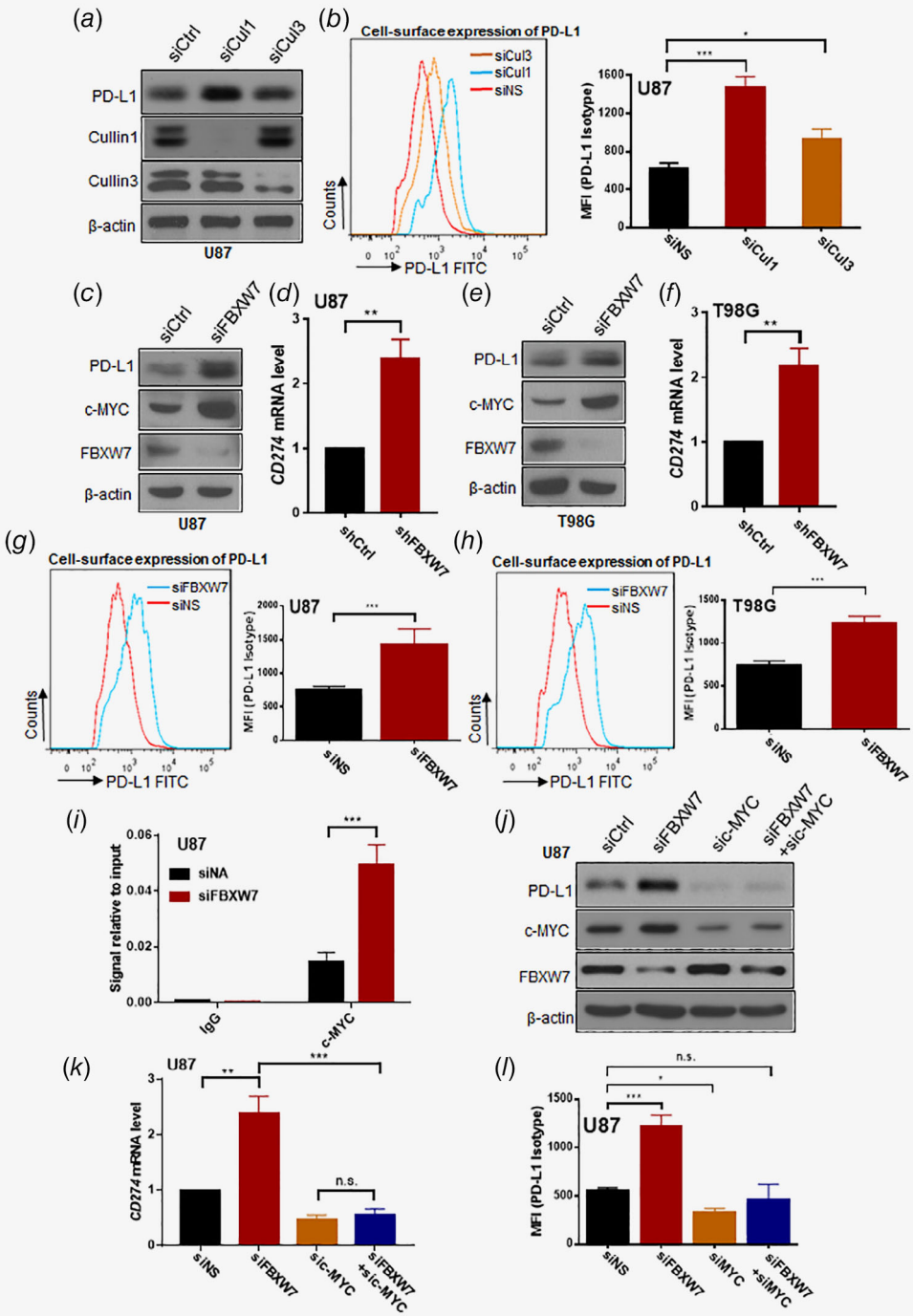

Figure 3. Neddylation inhibition-induced PD-L1 upregulation is mainly attributed by Cullin1-FBXW7/c-MYC axis. (*a*) U87 cells were transfected with siCullin1 or siCullin3 for 72 hr. The cell lysates were applied to SDS-PAGE for detection of PD-L1 proteins by immunoblotting. (*b*) Flow cytometry analysis and quantification of cell surface PD-L1 protein levels on the U87 cells with depletion of Cullin1 or Cullin3. (*c*, *e*) Immunoblotting analysis of c-MYC and PD-L1 expression in both U87 and T98G cells upon knockdown of E3 ubiquitin ligase FBXW7. (*d*, *f*) qPCR analysis of the *PD-L1* mRNA levels in both U87 and T98G cells upon knockdown of FBXW7. (*g*, *h*) U87 and T98G cells were treated with scramble or FBXW7 siRNA for 72 hr. The cells were harvested for flow cytometry analysis to detect and quantify cell surface PD-L1 protein levels. (*i*) ChIP assay to detect the physical interaction of c-MYC and *PD-L1* promoter region upon transfection of FBXW7 siRNA. (*j*) Co-transfection of c-MYC siRNA rescued FBXW7 silencing-induced upregulation of PD-L1 expression in U87 cells by immunoblotting analysis. (*k*) qPCR analysis of the *PD-L1* mRNA levels in U87 cells upon treatment of siCtrl, siFBXW7, *sic*-MYC or *sic*-MYC+siFBXW7. (*l*) Cell surface PD-L1 proteins were downregulated upon c-MYC siRNA co-transfection in U87 cells with depletion of FBXW7. [Color figure can be viewed at wileyonlinelibrary.com]

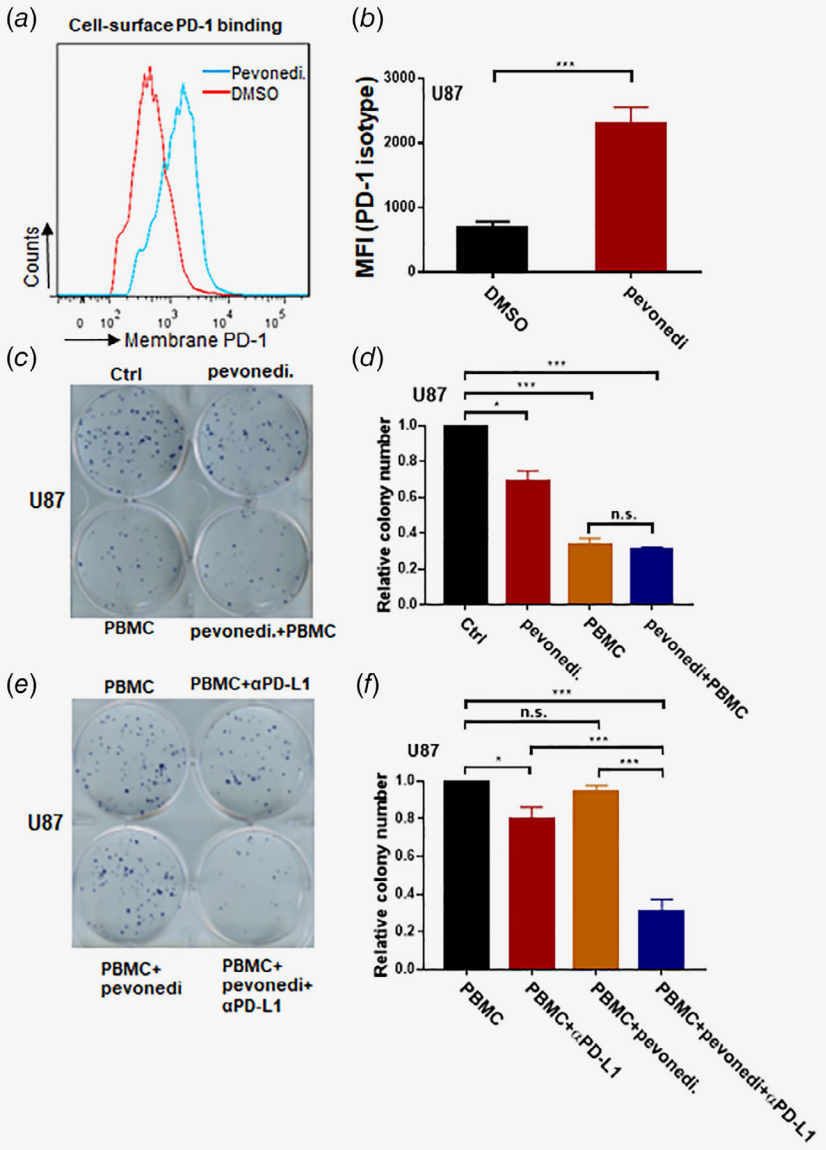

Figure 4. Pevonedistat attenuates T cell killing through PD-L1 induction. (*a*) FACS analysis of cell surface PD-1 binding of U87 cells upon treatment of 1 μM pevonedistat for 48 hr. (*b*) Quantification of PD-1 binding to cell surface of U87 cells treated with dimethyl sulfoxide or 1 μM pevonedistat. (*c*) U87 cells expressing RFP protein were first treated with or without pevonedistat (1 μM) for 12 hr and then cocultured with or without activated PBMCs. After 48 hr, U87-RFP cells were sorted by flow cytometry and applied for clonogenic assay. (*d*) Quantification of relative surviving colonies in the indicated four groups: control, pevonedistat treatment, PBMC treatment, co-treatment of pevonedistat and PBMC. (*e*) U87-RFP cells were treated with or without pevonedistat (1 μM) for 12 hr and then cocultured with activated PBMCs in the presence or absence of anti-PD-L1 antibody (10 μg/mL) for 48 hr. U87-RFP cells were then sorted by flow cytometry and applied for clonogenic assay. (*f*) Quantification of relative colony numbers in the indicated groups of (*e*). [Color figure can be viewed at wileyonlinelibrary.com]

of c-MYC silencing on FBXW7 knockdown-induced PD-L1 mRNA and protein upregulation was observed in T98G cells (Figs. S3*c*–S3*e*). Cullin3-SPOP E3 ligase is shown to be the physiological E3 ubiquitin ligase for PD-L1.[22] Consistent with this notion, we were also able to detect relatively lower intensity of polyubiquitinated PD-L1 signals in the cells treated with siCullin3 (Fig. S3*f*). Taken together, our results indicate that Cullin1-FBXW7/c-MYC axis contributes to the upregulation of PD-L1 expression in GBM cells.

Inhibition of neddylation pathway attenuates T cell killing through PD-L1 induction

In order to examine whether pevonedistat-induced PD-L1 upregulation has physiological function, we first explored the

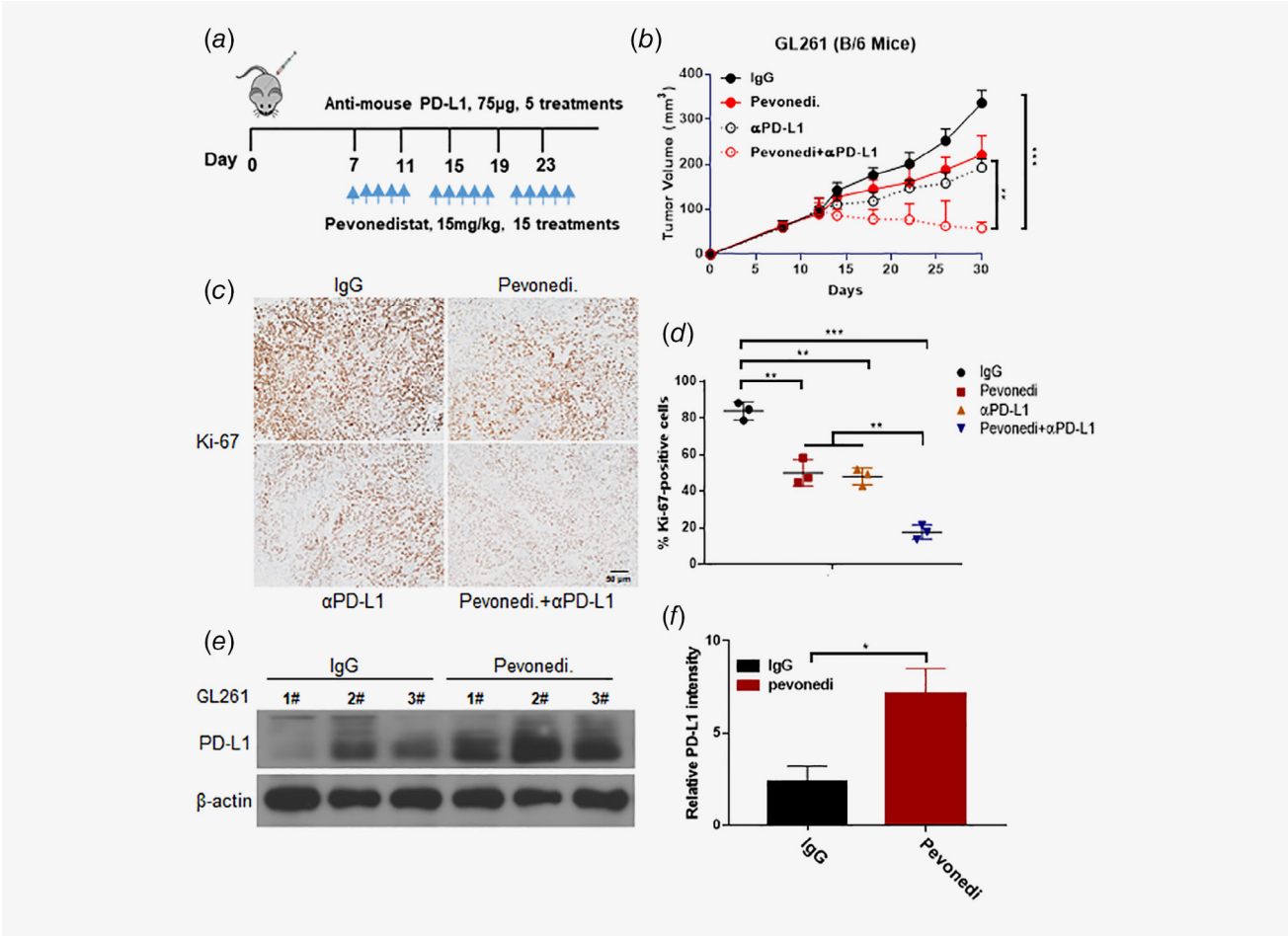

Figure 5. Pevonedistat-induced suppression of anticancer immunity is abrogated by PD-L1 blockade in vivo. (*a*) A schematic of the treatment plan for mice bearing subcutaneous GL261 tumors. Female C57BL/6 mice were implanted with 1×10^6 GL261 cells subcutaneously and received one of four treatments: control antibody treatment, pevonedistat treatment, anti-PD-L1 antibody treatment or anti-PD-L1 antibody plus pevonedistat combination treatment. (*b*) GL261 implanted tumor-bearing mice were randomly enrolled in different treatment groups as indicated. For each treatment group, tumor volumes were measured every 4 days and plotted individually. (*c*) Immunohistochemical Ki-67 staining and quantification of GL261 tumors in each treatment group. Scale bar, 50 μm. (*d*) Percentage quantification of Ki-67 positive cells in (*c*). (*e*) GL261 tumors from control and pevonedistat-treated groups were isolated to evaluate mouse PD-L1 protein expression by immunoblotting. (*f*) The intensity of mouse PD-L1 protein levels was quantified and plotted for control and pevonedistat-treated groups. [Color figure can be viewed at wileyonlinelibrary.com]

binding intensity of PD-1 on GBM cells. Upon incubation of recombinant PD-1 protein with U87 cells, the binding of PD-1 on the cell surface was significantly increased in the pevonedistat-treated cells compared to the control cells (Figs. 4*a* and 4*b*). We observed similar changes in T98G cells with pevonedistat treatment (Figs. S4*a* and S4*b*). The inhibitory signals mediated by PD-1 play a major role in T cell inactivation, exhaustion during cancer development.[27,28] We next sought to determine whether inhibition of neddylation pathway affects T cell function. To this end, we cocultured U87-RFP (red fluorescence) cells with activated human PBMCs in the presence or absence of pevonedistat. After 48 hr, the U87-RFP cells were sorted using flow cytometry and subjected to clonogenic formation assay. As expected, pevonedistat and T cells efficiently inhibited the clonogenic cell survival. Interestingly, U87-RFP cells co-administrated of both pevonedistat and T cells demonstrated similar surviving clones compared to PBMC treatment alone, indicating that pevonedistat treatment might block the cytolytic effect of T cells (Figs. 4*c* and 4*d*). Based on these results, we further explore the impact of the combination of anti-PD-L1 antibody and pevonedistat on the GBM cell survival in the PBMC-mediated cell killing assay. As shown in Figures 4*e* and 4*f*, blockade of PD-L1/PD-1 interaction by PD-L1 antibody sensitized pevonedistat-treated U87-RFP cells to activated PBMC-induced cell killing. Hence, these above results indicated that inhibition of neddylation pathway by pevonedistat in GBM cells mitigates T cell-mediated cell death, while PD-L1/PD-1 immune checkpoint inhibitors can reverse pevonedistat-induced immune resistance.

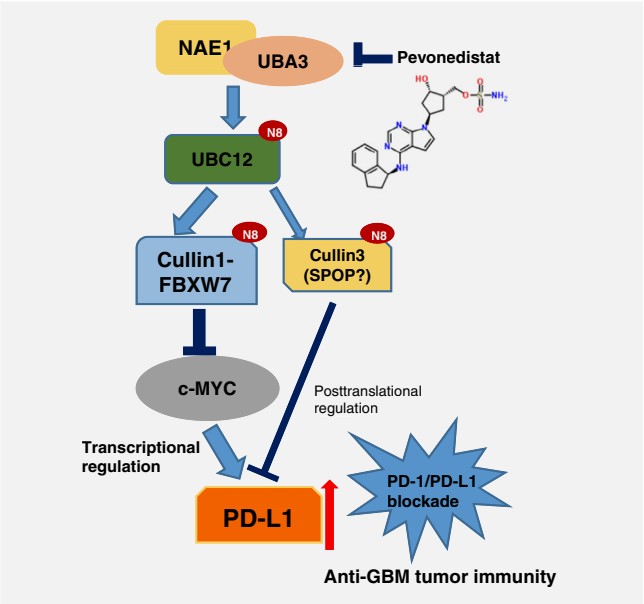

Figure 6. Synergistic effect of pevonedistat and PD-L1/PD-1 blockade in the treatment of GBM tumors. A working model of how PD-L1 protein level is regulated by the neddylation pathway in GBM cells. Genetic and pharmacologic inhibition of neddylation pathway upregulates PD-L1 expression largely through abrogating the E3 ubiquitin ligase activity of SKP1-Cullin1-FBXW7 complex, which thereby stabilize a key oncoprotein substrate c-MYC. C-MYC directly binds to the promoter region of *PD-L1* gene and transcriptionally activates *PD-L1* expression. At the same time, inhibition of neddylation pathway is able to attenuate Cullin3 ubiquitin ligase activity, which in turn prolongs the half-life of PD-L1 protein. Therefore, the rise in PD-L1 might be one of the underlying mechanisms accounting for pevonedistat resistance *via* evasion of immune surveillance checkpoints. Our work provides a molecular mechanism as well as the rationale for the combination of neddylation pathway inhibitor pevonedistat and PD-L1 blockade treatment as a more efficient anticancer therapeutic strategy in future. [Color figure can be viewed at wileyonlinelibrary.com]

Pevonedistat-induced suppression of anticancer immunity is abrogated by PD-L1 blockade *in vivo*

Clinical investigations showed that the efficacy of anti-PD-L1/PD-1 immunotherapy correlates with tumor cells-associated PD-L1 protein levels.[29,30] Given pevonedistat-induced PD-L1 upregulation in GBM tumor cells, we hypothesized that inhibition of neddylation pathway by pevonedistat might synergize with PD-L1 blockade to enhance therapeutic effect. We therefore treated immuno-proficient mice bearing GL261 tumors with pevonedistat and anti-PD-L1 alone or in combination (Fig. 5*a*). In line with our observations *in vitro*, pevonedistat plus PD-L1 blockade antibody markedly retarded GL261 tumor progression relative to the growth restriction by each agent alone (Fig. 5*b*). However, we did not find any obvious changes in body weight of these four different treatment groups (Fig. S5). Additionally, Ki-67 positive stained tumor cells were significantly fewer in the combined treatment group compared to each treatment alone (Figs. 5*c* and 5*d*). In line with the observation in Figure 2, mouse PD-L1 expression was significantly elevated upon pevonedistat treatment in this allograft mouse model (Figs. 5*e* and 5*f*), which further validated that protein neddylation inhibitor-mediated the PD-L1 upregulation is the molecular basis of this synergistic effect. These results suggested that PD-L1 blockade potentiates the therapeutic effect of pevonedistat by abrogating the acquired tumor-associated immunosuppression in GBM.

Discussion

As a promising anticancer agent, pevonedistat is currently in multiple Phase I/II clinical trials for both solid tumors and hematological malignancies.[31–34] Overactivation of the neddylation pathway has been observed in majority of samples in a GBM tumor cohort compared to normal tissues.[5] Inhibition of neddylation pathway by pevonedistat as a potential therapeutic strategy has been validated in both GBM cancer cells *in vitro* and an orthotopic xenograft mouse model *in vivo*.[5] In addition, pevonedistat might have its advantage over other agents regarding penetrating the blood brain barrier, since pevonedistat is a small molecule inhibitor with low molecular weight and high solubility in lipid. Although the cytotoxic effects of pevonedistat, including inducing cell-cycle arrest, apoptosis and autophagy, have been well studied, the role of neddylation inhibition in cancer-associated immunity remains largely unknown. Glioblastoma usually establishes an immunosuppressive tumor microenvironment in the brain, which helps the lesion growth and become malignant through evading immune system.[35–37] Thus, immunotherapy to counteract immune evasion and suppression has already been underway in a few preclinical and clinical studies in GBM.[18,38–40] The scientific basis from our study is able to help testing the efficacy of the combination of pevonedistat and PD-L1/PD-1 antibody in GBM by leveraging the advantages of two powerful anticancer agents. Thus, the synergistic effect of pevonedistat and anti-PD-L1/PD-1 needs to be investigated in an orthotopic model in future studies.

Our studies suggest that simultaneous inhibition of neddylation pathway and PD-L1 may benefit GBM patients. Therefore, the highly active status of the neddylation pathway in GBM patients might serve as a biomarker for the standard of patient population enrollment in clinical trials for the combination treatment of pevonedistat and immune checkpoint inhibitors. Moreover, our results also indicate that inhibition of Cullin1-SKP1-FBXW7 E3 ligase activity and thereby accumulation of c-MYC protein by pevonedistat leads to PD-L1 upregulation (Fig. 6). Therefore, the expression levels or mutation status of FBXW7 and c-MYC proteins might also reflect the therapeutic efficacy of the combination treatment. Indeed, both loss-of-function (mutations or deletion) of tumor suppressor FBXW7 and overexpression of c-MYC oncoprotein correlate with PD-L1 expression levels and poor prognosis in some malignancies.[41,42] Therefore, whether anti-PD-L1/PD-1 immunotherapy induces better effect in GBM patients with FBXW7 inactivation and/or MYC activation remains further investigation.

Inhibition of neddylation by pevonedistat has been shown to suppress the release of some proinflammatory cytokines by dendritic cells such as TNF-α and IL-6, and mitigates dendritic

cells-mediated T cell stimulation.[43] However, in our study, we could observe PD-L1 blockade potentiates pevonedistat *in vitro* and *in vivo*, indicating that anti-PD-L1 successfully reverses pevonedistat-induced T cell inactivation. Careful attention should be paid to the dose and dosing regimen in future studies to prevent "over-inhibition" of T cell function by pevonedistat. Taken together, the interaction between neddylation pathway and PD-L1 as shown in our study is timely for developing more effective combination therapies in GBM.

In summary, we in our study demonstrated that pevonedistat markedly upregulates PD-L1 expression primarily through inactivation of Cullin1 and Cullin3 activity, which in turn transcriptionally drives PD-L1 gene expression by dysregulated Cullin1-FBXW7/c-MYC axis and stabilizes PD-L1 protein by decreased Cullin3 E3 ubiquitin ligase activity. Therefore, pevonedistat renders GBM cells more resistant to cytolysis induced by T cells, whereas blockade of PD-L1 successfully potentiates pevonedistat *in vitro* and *in vivo*. The results of this work provided a scientific rationale for clinical trials of coadministration of pevonedistat and anti-PD-L1/PD-1 in GBM patients in future.

Author Contributions

Conception and design: Zhang Q, Wang X; Development of methodology: Zhou S, Zhao X, Yang Z, Yang R, Chen C, Zhao K, Wang W, Ma Y; Acquisition of data: Zhou S, Zhao X, Yang Z, Yang R, Chen C, Zhao K, Ma Y; Analysis and interpretation of data: Zhou S, Zhao X, Yang Z, Wang W, Ma Y, Zhang Q, Wang X; Writing and review of the manuscript: Zhou S, Zhao X, Yang Z, Zhang Q, Wang X; Technical or material support: Yang R, Chen C, Zhao K, Wang W, Ma Y; Study supervision: Zhang Q, Wang X.

References

1. Ajaz M, Jefferies S, Brazil L, et al. Current and investigational drug strategies for glioblastoma. *Clin Oncol (R Coll Radiol)* 2014;26:419–30.
2. Delgado-Lopez PD, Corrales-Garcia EM. Survival in glioblastoma: a review on the impact of treatment modalities. *Clin Transl Oncol* 2016;18:1062–71.
3. Enchev RI, Schulman BA, Peter M. Protein neddylation: beyond cullin-RING ligases. *Nat Rev Mol Cell Biol* 2015;16:30–44.
4. Watson IR, Irwin MS, Ohh M. NEDD8 pathways in cancer, Sine Quibus Non. *Cancer Cell* 2011;19:168–76.
5. Hua W, Li C, Yang Z, et al. Suppression of glioblastoma by targeting the overactivated protein neddylation pathway. *Neuro Oncol* 2015;17:1333–43.
6. Soucy TA, Smith PG, Milhollen MA, et al. An inhibitor of NEDD8-activating enzyme as a new approach to treat cancer. *Nature* 2009;458:732–6.
7. Soucy TA, Smith PG, Rolfe M. Targeting NEDD8-activated cullin-RING ligases for the treatment of cancer. *Clin Cancer Res* 2009;15:3912–6.
8. Wei D, Li H, Yu J, et al. Radiosensitization of human pancreatic cancer cells by MLN4924, an investigational NEDD8-activating enzyme inhibitor. *Cancer Res* 2012;72:282–93.
9. Li H, Zhou W, Li L, et al. Inhibition of neddylation modification sensitizes pancreatic cancer cells to gemcitabine. *Neoplasia* 2017;19:509–18.
10. Garcia K, Blank JL, Bouck DC, et al. Nedd8-activating enzyme inhibitor MLN4924 provides synergy with mitomycin C through interactions with ATR, BRCA1/BRCA2, and chromatin dynamics pathways. *Mol Cancer Ther* 2014;13:1625–35.
11. Cooper J, Xu Q, Zhou L, et al. Combined inhibition of NEDD8-activating enzyme and mTOR suppresses NF2 loss-driven tumorigenesis. *Mol Cancer Ther* 2017;16:1693–704.
12. Swords RT, Coutre S, Maris MB, et al. Pevonedistat, a first-in-class NEDD8-activating enzyme inhibitor, combined with azacitidine in patients with AML. *Blood* 2018;131:1415–24.
13. Zou W, Wolchok JD, Chen L. PD-L1 (B7-H1) and PD-1 pathway blockade for cancer therapy: mechanisms, response biomarkers, and combinations. *Sci Transl Med* 2016;8:328rv4.
14. Zou W, Chen L. Inhibitory B7-family molecules in the tumour microenvironment. *Nat Rev Immunol* 2008;8:467–77.
15. Topalian SL, Hodi FS, Brahmer JR, et al. Safety, activity, and immune correlates of anti-PD-1 antibody in cancer. *N Engl J Med* 2012;366:2443–54.
16. Hargadon KM, Johnson CE, Williams CJ. Immune checkpoint blockade therapy for cancer: an overview of FDA-approved immune checkpoint inhibitors. *Int Immunopharmacol* 2018;62:29–39.
17. Nduom EK, Wei J, Yaghi NK, et al. PD-L1 expression and prognostic impact in glioblastoma. *Neuro Oncol* 2016;18:195–205.
18. Roth P, Valavanis A, Weller M. Long-term control and partial remission after initial pseudoprogression of glioblastoma by anti-PD-1 treatment with nivolumab. *Neuro Oncol* 2017;19:454–6.
19. Galluzzi L, Buque A, Kepp O, et al. Immunological effects of conventional chemotherapy and targeted anticancer agents. *Cancer Cell* 2015;28:690–714.
20. Patel SA, Minn AJ. Combination cancer therapy with immune checkpoint blockade: mechanisms and strategies. *Immunity* 2018;48:417–33.
21. Topalian SL, Drake CG, Pardoll DM. Targeting the PD-1/B7-H1(PD-L1) pathway to activate anti-tumor immunity. *Curr Opin Immunol* 2012;24:207–12.
22. Zhang J, Bu X, Wang H, et al. Cyclin D-CDK4 kinase destabilizes PD-L1 via cullin 3-SPOP to control cancer immune surveillance. *Nature* 2018;553:91–5.
23. Milhollen MA, Thomas MP, Narayanan U, et al. Treatment-emergent mutations in NAEbeta confer resistance to the NEDD8-activating enzyme inhibitor MLN4924. *Cancer Cell* 2012;21:388–401.
24. Duda DM, Borg LA, Scott DC, et al. Structural insights into NEDD8 activation of cullin-RING ligases: conformational control of conjugation. *Cell* 2008;134:995–1006.
25. Zhao Y, Morgan MA, Sun Y. Targeting Neddylation pathways to inactivate cullin-RING ligases for anticancer therapy. *Antioxid Redox Signal* 2014;21:2383–400.
26. Casey SC, Tong L, Li Y, et al. MYC regulates the antitumor immune response through CD47 and PD-L1. *Science* 2016;352:227–31.
27. Thommen DS, Schumacher TN. T cell dysfunction in cancer. *Cancer Cell* 2018;33:547–62.
28. Catakovic K, Klieser E, Neureiter D, et al. T cell exhaustion: from pathophysiological basics to tumor immunotherapy. *Cell Commun Signal* 2017;15:1.
29. Herbst RS, Soria JC, Kowanetz M, et al. Predictive correlates of response to the anti-PD-L1 antibody MPDL3280A in cancer patients. *Nature* 2014;515:563–7.
30. Iwai Y, Ishida M, Tanaka Y, et al. Involvement of PD-L1 on tumor cells in the escape from host immune system and tumor immunotherapy by PD-L1 blockade. *Proc Natl Acad Sci U S A* 2002;99:12293–7.
31. Shah JJ, Jakubowiak AJ, O'Connor OA, et al. Phase I study of the novel investigational NEDD8-activating enzyme inhibitor pevonedistat (MLN4924) in patients with relapsed/refractory multiple myeloma or lymphoma. *Clin Cancer Res* 2016;22:34–43.
32. Sarantopoulos J, Shapiro GI, Cohen RB, et al. Phase I study of the investigational NEDD8-activating enzyme inhibitor pevonedistat (TAK-924/MLN4924) in patients with advanced solid tumors. *Clin Cancer Res* 2016;22:847–57.
33. Lockhart AC, Bauer TM, Aggarwal C, et al. Phase Ib study of pevonedistat, a NEDD8-activating enzyme inhibitor, in combination with docetaxel, carboplatin and paclitaxel, or gemcitabine, in patients with advanced solid tumors. *Invest New Drugs* 2018;37:87–97.
34. Zhou L, Zhang W, Sun Y, et al. Protein neddylation and its alterations in human cancers for targeted therapy. *Cell Signal* 2018;44:92–102.
35. Lim M, Xia Y, Bettegowda C, et al. Current state of immunotherapy for glioblastoma. *Nat Rev Clin Oncol* 2018;15:422–42.
36. Chae M, Peterson TE, Balgeman A, et al. Increasing glioma-associated monocytes leads to increased intratumoral and systemic myeloid-derived suppressor cells in a murine model. *Neuro Oncol* 2015;17:978–91.
37. Schiffer D, Mellai M, Bovio E, et al. The neuropathological basis to the functional role of microglia/macrophages in gliomas. *Neurol Sci* 2017;38:1571–7.
38. Reardon DA, Gokhale PC, Klein SR, et al. Glioblastoma eradication following immune

checkpoint blockade in an orthotopic, immunocompetent model. *Cancer Immunol Res* 2016;4:124–35.
39. Bouffet E, Larouche V, Campbell BB, et al. Immune checkpoint inhibition for hypermutant glioblastoma multiforme resulting from germline biallelic mismatch repair deficiency. *J Clin Oncol* 2016;34:2206–11.
40. Johanns TM, Miller CA, Dorward IG, et al. Immunogenomics of hypermutated glioblastoma: a patient with germline POLE deficiency treated with checkpoint blockade immunotherapy. *Cancer Discov* 2016;6:1230–6.
41. Aydin IT, Melamed RD, Adams SJ, et al. FBXW7 mutations in melanoma and a new therapeutic paradigm. *J Natl Cancer Inst* 2014;106:dju107.
42. Kim EY, Kim A, Kim SK, et al. MYC expression correlates with PD-L1 expression in non-small cell lung cancer. *Lung Cancer* 2017;110:63–7.
43. Mathewson N, Toubai T, Kapeles S, et al. Neddylation plays an important role in the regulation of murine and human dendritic cell function. *Blood* 2013;122:2062–73.